THE JOURNAL OF BIOLOGICAL CHEMISTRY VOL. 284, NO. 52, pp. 36271–36281, December 25, 2009

Regulation of Iron Homeostasis in *Arabidopsis thaliana* by the Clock Regulator Time for Coffee*[S]

Received for publication, August 26, 2009, and in revised form, October 9, 2009 Published, JBC Papers in Press, October 14, 2009, DOI 10.1074/jbc.M109.059873

Céline Duc[‡1], Françoise Cellier[‡], Stéphane Lobréaux[§], Jean-François Briat[‡], and Frédéric Gaymard[‡2]

From the [‡]Laboratoire de Biochimie et Physiologie Moléculaire des Plantes, UMR 5004, Agro-M/CNRS/Institut National de la Recherche Agronomique/Université Montpelier II, 34060 Montpellier Cedex 1 and the [§]Laboratoire Plastes et Différenciation Cellulaire, Universite Joseph Fourier Grenoble 1, Centre de Recherche sur les Macromolécules Organisées, BP 53, 38041 Grenoble Cedex 9, France

In plants, iron homeostasis is tightly regulated to supply sufficient amounts of this metal for an optimal growth while preventing excess accumulation to avoid oxidative stress. To identify new regulators of iron homeostasis, a luciferase-based genetic screen using the *Arabidopsis AtFer1* ferritin promoter as a target was developed. This screen identified TIME FOR COFFEE (TIC) as a regulator of *AtFer1* gene expression. TIC was previously described as a nuclear regulator of the circadian clock. Mutants in the *TIC* gene exhibited a chlorotic phenotype rescued by exogenous iron addition and are hypersensitive to iron during the early stages of development. We showed that iron overload-responsive genes are regulated by TIC and by the central oscillator of the circadian clock. TIC represses their expression under low iron conditions, and its activity requires light and light/dark cycles. Regarding *AtFer1*, this repression is independent of the previously characterized *cis*-acting element iron-dependent regulatory sequence, known to be involved in *AtFer1* repression. These results showed that the regulation of iron homeostasis in plants is a major output of the TIC- and central oscillator-dependent signaling pathways.

Iron is an essential element for all organisms. However, its physiological concentration needs to be tightly regulated because of its high reactivity with oxygen (1). The regulatory mechanisms controlling iron homeostasis in bacteria and animals are well documented (2, 3), in contrast with the lack of knowledge in plants.

This last decade, a wealth of information has been obtained on the molecular characterization of genes involved in iron acquisition by roots, in iron allocation to various organs, and in subcellular compartmentalization of iron in plants (reviewed in Refs. 4 and 5). The present challenge in this field concerns our understanding of the integration of these functions at the whole plant level and the signaling networks and regulatory molecules responsible for the control of iron dynamics in plants. Although the iron regulation of genes involved in uptake and storage has been widely studied, only a few components of the iron signaling pathway are known. Furthermore, studies regarding this aspect have, up until now, focused on the identification of regulatory proteins that function in the iron deficiency signaling pathway (reviewed in Refs. 6 and 7). Hence, genes involved in iron excess signaling pathways have yet to be identified in plants. One of the primary responses to iron excess is a quick accumulation of a large amount of ferritins in plastids (reviewed in Ref. 6). Ferritins play an essential role in iron homeostasis by sequestering iron in a bio-available and nontoxic form, thus preventing oxidative stress (8). Among the four ferritin genes of *Arabidopsis thaliana*, *AtFer1* is the most highly expressed in response to iron excess (8), making it an ideal model for studying iron homeostasis regulation. Furthermore, *AtFer1*-transcriptional regulation by the iron status occurs through a repression/derepression mechanism. Experiments based on serial deletions and site-directed mutagenesis of the *AtFer1* ferritin promoter region allowed the identification of a 15-bp *cis*-acting element necessary for the iron-dependent regulation of the *AtFer1* transcription (9). This sequence, named iron-dependent regulatory sequence (IDRS),[3] is involved in the repression of *AtFer1* expression under iron deficiency (9, 10). Thus, iron addition leads to the derepression of *AtFer1* rather than to its induction. To identify components of the iron signaling pathway, we screened for mutants impaired in the *AtFer1* repression/derepression in response to iron status. We used a p*AtFer1*::*LUC* reporter line to identify ethyl methanesulfonate (11) mutants in *Arabidopsis* harboring a high LUC activity under repressive conditions, *i.e.* low iron. Two mutants, exhibiting a high LUC activity and a 10-fold increase in *AtFer1* mRNA accumulation compared with wild type plants, were isolated and named *dif3* and *dif6* (deregulated in ferritin). They were allelic and mutated in the *TIC* (*Time for Coffee*) gene, which encodes a nuclear regulator of the circadian clock (12, 13). We showed that the mutation in *TIC* led to the derepression of *AtFer1* under repressive conditions. The TIC-mediated *AtFer1* regulation was circadian clock-dependent and did

* This work was supported by the Institut National de la Recherche Agronomique, the CNRS, and Action Concertée Incitative "Biologie Cellulaire Moléculaire et Structurale" Grant BCMS166 from the Ministère de l'Education Nationale, de l'Enseignement Supérieur et de la Recherche.

[S] The on-line version of this article (available at http://www.jbc.org) contains supplemental Table S1 and Figs. S1–S3.

[1] Recipient of a thesis fellowship supported by Région Languedoc-Roussillon and Institut National de la Recherche Agronomique.

[2] To whom correspondence should be addressed: 2 place Viala, 34060 Montpellier Cedex 1, France. Tel.: 33-499-612-932; Fax: 33-467-525-737; E-mail: gaymard@supagro.inra.fr.

[3] The abbreviations used are: IDRS, iron-dependent regulatory sequence; Q-PCR, quantitative PCR; RTL, relative transcript level; LUC, luciferase; LD, light/dark; LL, continuous light; EMS, ethylmethane sulfonate.

not occur through the *cis*-element IDRS. Our results showed that TIC and a functional central oscillator of the circadian clock are required for the expression of iron-regulated genes. This work points out that when plants do not experience iron excess, iron homeostasis is regulated through a circadian clock-dependent pathway, leading to the modulation of iron-responsive genes.

EXPERIMENTAL PROCEDURES

Plant Material—The wild type *A. thaliana* ecotypes used were Columbia-0 (Col) and Wassilevskija (Ws). The mutants *dif3*, *dif6*, and *tic*-2 were in the Col genetic background; *tic-1*, *elf4-1*, *cca1-11*, and *lhy-21* were in the Ws genetic background.

Growth Conditions—For hydroponic cultures, the plants were grown for 6 weeks in a growth chamber (250 μmol·m^{-2}·s^{-1}, relative humidity 70%, 8 h of light at 23 °C/16 h of dark at 20 °C). The seeds were sown on wet sand laid on a polystyrene raft floating on water. After 2 weeks on water, the rafts were transferred to a nutrient solution containing the following elements: 0.5 mM KNO_3, 0.25 mM $Ca(NO_3)_2$, 1 mM $MgSO_4$, 1 mM KH_2PO_4, 100 μM Fe(III)-Na-EDTA, 50 μM H_3BO_3, 19 μM $MnCl_2$, 1 μM $CuSO_4$, 10 μM $ZnCl_2$, 0.02 μM MoO_4Na_2, pH 5.8. The nutrient solutions were renewed every week. The treatments were performed on 6-week-old plants. For iron deficiency treatment, the roots were washed twice with 0.3 mM bathophenanthroline disulfonic acid and 5.7 mM $Na_2S_2O_4$ to remove apoplasmic iron. Then the rafts were transferred to the initial nutrient solution but without iron added. Iron overload treatment was performed after 1 week of culture in the iron-deficient medium, by adding 500 μM iron citrate for 5 h (14). In a greenhouse, the plants were grown on Humin substrate N2 (Neuhaus, Klasmann-Deilmann, Germany) at 23 °C, with a sunlight intensity limited to 300 μmol·m^{-2}·s^{-1} and 16 h of light/8 h of dark.

For *in vitro* culture, the seeds were surface-sterilized by soaking in a solution containing Bayrochlor 1.5% (w/v) (Indusco France) and ethanol 50% for 30 min under agitation, rinsed three times in ethanol, and dried overnight under a sterile air flow. Sterilized seeds were sown on plates containing a half Murashige and Skoog standard medium (Sigma M0654) supplemented with 100 μM H_3BO_3, 100 μM $MnSO_4$, 30 μM $ZnSO_4$, 5 μM KI, 1 μM Na_2MoO_4, 0.11 μM $CoCl_2$, 0.10 μM $CuSO_4$, 0.5 g·liter^{-1} 2-morpholinoethane sulfonic acid (Sigma), 1% (w/v) sucrose (Sigma), 7 g·liter^{-1} agar, pH 5.8. The plates were placed in a growth chamber (300 μmol·m^{-2}·s^{-1}, relative humidity 70%, 16 h of light at 23 °C/8 h of dark at 20 °C). Ferrozine (3-(2-pyridinyl)-5,6-diphenyl-1,2,4-triazine-4′,4″-disulfonic acid sodium salt) was added at a final concentration of 200 μM for short term iron deficiency. A solution of 500 μM iron citrate was sprayed on plants for short term iron excess experiments.

Circadian Phase Response Analysis—The plantlets were entrained on soil for 2 weeks in 16 h of light/8 h of dark conditions in a growth chamber (20 °C, 250 μmol·m^{-2}·s^{-1}) and then moved into continuous light or kept in 16 h of light/8 h of dark. Triplicate samples were harvested every 4 h for Q-PCR analysis.

Dark-induced Response Analysis—The plantlets were entrained on soil for 2 weeks in 16 h of light/8 h of dark conditions in a growth chamber (20 °C, 250 μmol·m^{-2}·s^{-1}) and then moved into continuous darkness for 3 days. *T*0 was 30 min before the transfer and the lighting. Each day, the triplicate samples were harvested 30 min before the subjective dawn for Q-PCR analysis. The third day, at the subjective dawn, the plants were put back in the initial growth chamber (20 °C, 250 μmol·m^{-2}·s^{-1}), and triplicate samples were collected 1, 3, and 5 h after transfer.

Mutant Screening and Map-based Cloning—A transgenic line, carrying the promoter of *AtFer1* fused to the LUC reporter gene, was used for mutant screening. The NheI/XbaI-digested *luc*+ fragment, excised from the pSP-luc+ vector (Promega, WI), was inserted into the SpeI/XbaI-digested pBluescript II KS+ (pKS+, Stratagene). Afterward, the SalI/NcoI-digested fragment of the *At1400IDRS* construct (9) was inserted into the pKS-*luc*+. The resulting *At1400IDRS-luc*+ fragment was finally inserted into the KpnI/SacI-digested pMOG402 vector (MOGEN International). The resulting vector was introduced into *Agrobacterium tumefasciens* GV3101 strain and used to transform *A. thaliana* using the floral dip method (15). A mono-insertional and homozygous line was selected. Approximately 20,000 M1 seeds were mutagenized with 0.3% EMS for 10 h at 25 °C and sown on soil in a greenhouse. M2 seeds were collected in pools of 200 M1 plants. For the screening, 13-day-old M2 seedlings grown *in vitro* were sprayed with 1 mM luciferin (Promega) in 0.01% Triton X-100 and assayed for LUC bioluminescence using a CCD camera system (Hamamatsu C4880, Hamamatsu Photonics K.K., Joko, Japon). Bioluminescence images were processed using the software HiPic32 (Hamamatsu Photonics).

The rough mapping was performed thanks to markers described by Montpellier Institut National de la Recherche Agronomique and the Arabidopsis Information Resource. The fine mapping was performed by using tuned markers from the Marker Tracker data base at the University of Toronto. Genomic DNA from *dif3* mutant plants was extracted, and the mapped region was amplified by PCR as a set of 1 kbp of DNA fragments, each contiguous fragment overlapping on 150 bp. These DNA fragments were sequenced. The obtained nucleotide sequences were assembled with the SeqMan software (DNASTAR, Lasergene) and then aligned with the Col wild type DNA sequence to determine the mutation positions.

T-DNA Insertion Mapping—SAIL_753_E03 (*tic-2*) harbors a T-DNA insertion that was localized in the fourth exon of *TIC* after sequencing of the PCR product using the T-DNA-specific primer LB3A and the *TIC*-specific primers S31-F and S31-R. The p*AtFer1*::*LUC* transgene was mapped to chromosome 4 by thermal asymmetric interlaced PCR (16) in the intergenic region between At4g14820 and At4g14830 (data not shown). The position was confirmed by sequencing with LW-AD2, P1, and P2 primers. The insertion of the *At1400m*IDRS*:*GUS* was similarly recovered in the At2g38120 gene with LW-AD2 and P3-R primers. All of the primers used are presented in supplemental Table S1. For the *cca1-11* and *lhy-21* mutants, primer pairs were designed along the *CCA1* and *LHY* genomic sequence. Each primer pair was combined with the left border primer, specific of the T-DNA (JL202). The CCA1–2F/JL202 and LHY-3R/JL202 produced amplification, and their PCR

products were subsequently sequenced to confirm the insertion. The T-DNA location is presented in supplemental Fig. S2.

AtFer1 Overexpressing Line—The coding sequence of the mature AtFER1 protein (17) was digested BamHI/SacI and then inserted into the pSC51 vector. To obtain the pSC51 vector, the EcoRI/BamH1/BamI-digested *GUS* reporter gene fused to the *NOS* terminator was excised from the pBI121 (GenBank™ accession number AF485783) and cloned into the pMOG402 vector. The resulting vector was named pMOG-GUSt, and a 35S promoter was inserted into this vector by a SacI/HindII digestion, thus creating the pSC51 vector. The pSC51 vector with the *AtFer1* fragment was introduced into *A. tumefasciens* as described for the p*AtFer1*::*LUC* construct. Homozygous and mono-insertional lines were selected, and a line exhibiting a high *AtFer1* mRNA accumulation was chosen and named p35*S*::*AtFer1* Col.

RNA Isolation and Q-PCR—RNAs were isolated from rosettes or roots with the TRIzol reagent according to the manufacturer's instructions (Invitrogen). A DNase (Promega) treatment was performed on 5 μg of total RNAs to prevent genomic DNA contamination. RNA samples were subsequently used for reverse transcription (Moloney murine leukemia virus reverse transcriptase; Promega) with anchored oligo(dT)$_{15}$ (Promega) and dNTPs 0.4 mM. The cDNAs were diluted twice with water, and 1 μl of each cDNA sample was assayed by Q-PCR in a LightCycler (Roche Applied Science) using FastStart DNA Master PLUS Syber Green I (Roche Applied Science). The amplification efficiency was assessed relative to a sample standard. Expression levels were calculated relatively to the appropriate housekeeping gene (HK) using the comparative threshold cycle method, where C_t represented the threshold cycle for target amplification: $\Delta C_t = C_{t,\text{gene of interest}} - C_{t,HK}$ and the relative transcript level (RTL) was calculated as follow: $RTL = 10 \times 2^{-\Delta C_t}$. The primers are presented in supplemental Table S1.

Immunodetection of Ferritins—Five microliters of buffer (50 mM Tris-HCl, 5% (v/v) SDS, 0.72 M β-mercaptoethanol, 1 mM phenylmethylsulfonyl fluoride, 25 mM EDTA, 0.1% (w/v) bathophenanthroline disulfonic acid) were added per mg of plant tissue fresh weight. After 15 min at 4 °C, the samples were centrifuged for 30 min at 13,000 × *g*. Protein content was measured using bovine serum albumin as a standard (18). The protein samples were resolved by electrophoresis in an SDS-13% polyacrylamide gel (19) and then electroblotted onto polyvinylidene difluoride Hybond-P (Amersham Biosciences). Ferritin immunodetection was performed using a rabbit polyclonal antiserum raised against AtFER1 (17) recognizing the four ferritin subunits (8) and the Immobilon Western blotting kit (Millipore). A loading control was performed on a Coomassie Blue gel (Brilliant Blue R concentrate; Sigma).

LUC Reporter Gene Activity—The samples were grounded, suspended in 300 μl of 100 mM Na_2HPO_4 and centrifuged at 13,000 × *g*. Fifty microliters of Steady-Glo luciferase assay system (Promega) was added to 50 μl of protein extract supernatant. LUC activity was measured for 1 s after a 15-min incubation at room temperature and normalized to protein concentration, quantified with Bradford reagent (Bio-Rad) using bovine serum albumin as a standard.

Determination of Photosynthetic Pigment Content—The total pigment content was measured at 644.8, 661.6, and 470 nm after extraction with 2 ml of acetone for 50 mg of ground tissues (20). The pigment content was calculated as follows.

$$\text{Chl } a + b\ (\mu g \cdot ml^{-1}) = 7.05\, A_{661.6} + 18.09\, A_{644.8} \quad \text{(Eq. 1)}$$

$$\text{Chl } a\ (\mu g \cdot ml^{-1}) = 11.24\, A_{661.6} - 2.04\, A_{644.8} \quad \text{(Eq. 2)}$$

$$\text{Chl } b\ (\mu g \cdot ml^{-1}) = -4.19\, A_{661.6} + 20.13\, A_{644.8} \quad \text{(Eq. 3)}$$

$$\text{Carotenoides}\ (\mu g \cdot ml^{-1}) = (1000\, A_{470} - 1.9\ \text{Chla} - 63.14\ \text{Chlb})/214 \quad \text{(Eq. 4)}$$

Determination of Iron Content—The measurement of total iron content was performed as previously described (21). The samples were mineralized (22), and iron concentration was measured by the absorbance of 1% Fe^{2+}-bathophenanthroline disulfonic acid at 535 nm using thioglycolic acid (Sigma) as a reducing agent. Determination of iron content was performed using a range of a standard iron solution (Carlo Erba).

RESULTS

Identification of A. thaliana Mutants Affected in the Regulation of the AtFer1 Ferritin Gene—To identify genes involved in the transcriptional regulation of *AtFer1* in response to iron, transgenic lines in the Col-0 background carrying the *AtFer1* promoter fused to the *LUC* reporter gene were produced for the screen. Because *AtFer1* has been shown to be repressed in low iron conditions (9) and derepressed upon iron addition, the first genetic screen we performed aimed at identifying mutants derepressed under low iron conditions. A transgenic line exhibiting the lowest LUC activity under low iron, *i.e.* the highest repression of the promoter activity, was selected for EMS mutagenesis. The screening was performed on plants grown on a medium with low iron concentration (10 μM iron-EDTA). Candidate mutants harboring a high LUC bioluminescence were transferred on soil to obtain M3 seeds. The LUC phenotype was confirmed in the M3 progeny, and the candidate mutants were validated by selecting those overaccumulating the endogenous *AtFer1* mRNAs under low iron conditions. Confirmed mutants were named *dif* (deregulated in ferritin). Among the eight mutants identified, the mutant line *dif3*, exhibiting a high LUC expression, was selected for further analysis. This mutant line was backcrossed with a transgenic line. The segregation of the F2-progeny demonstrated that the mutant phenotype is caused by a recessive mutation independent of the reporter gene. For map-based cloning of the mutation, a *dif3* plant of the M4 progeny was crossed with Ler. Genomic DNA was prepared from the LUC-positive class (n = 220) of the F2 population (n = 1250) from this out-cross. Using cleaved-amplified polymorphic sequence and simple sequence length polymorphism markers, *dif3* was mapped to the upper arm of chromosome 3 at 28 centiMorgan on the *Arabidopsis* genetic map, between the simple sequence length polymorphism marker CER464947 and the cleaved-amplified polymorphic sequence marker Arlim15.1 (Fig. 1*A*). Afterward, for fine mapping, additional cleaved-amplified polymorphic sequence markers were used to surround the *dif3* mutation into a 136-

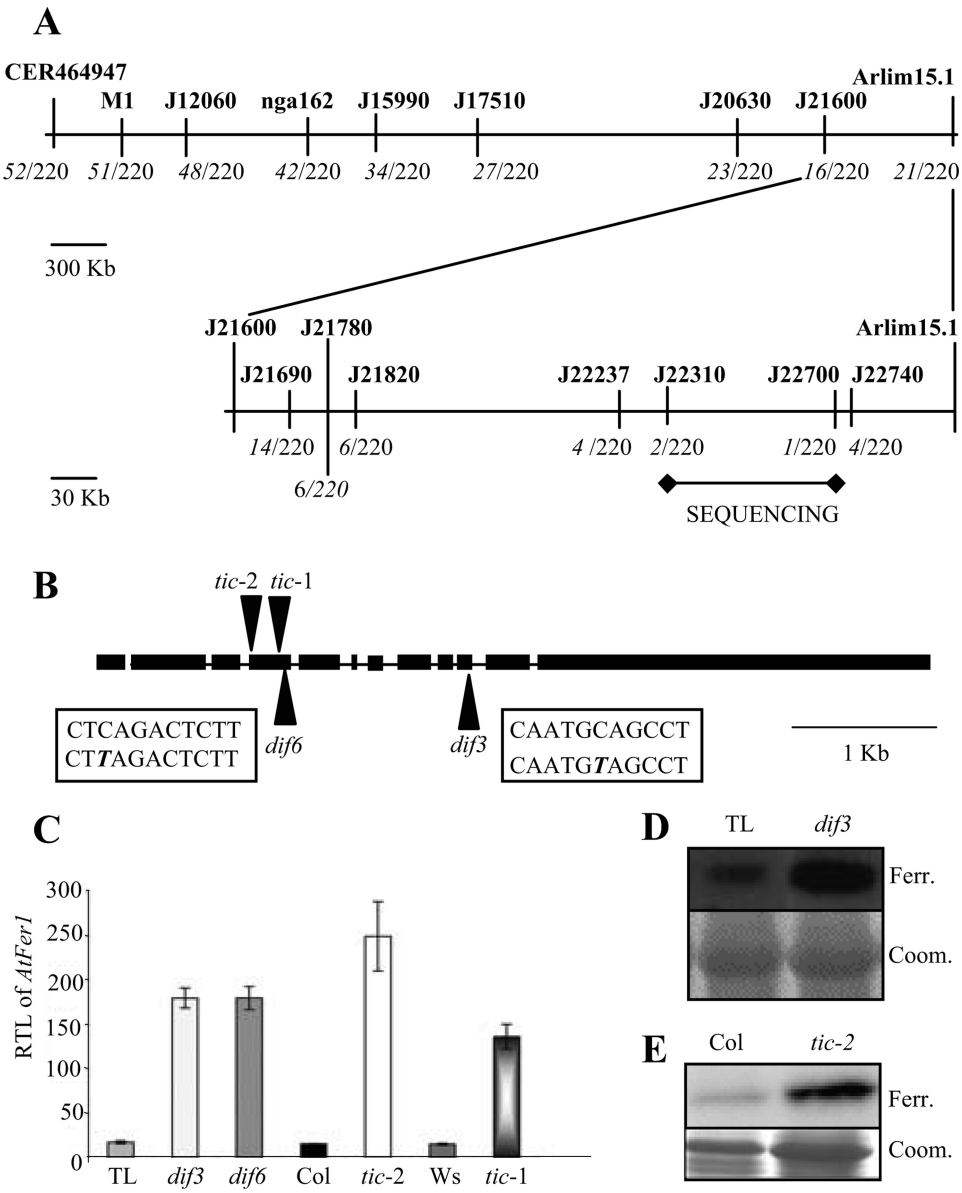

FIGURE 1. **Identification of *A. thaliana* mutants affected in ferritin regulation.** *A*, map-based cloning of *dif3*. The marker names are in *bold type*. The JXXXXX nomenclature indicates that the corresponding marker was designed in the At3gXXXXX gene (Marker Tracker). The number of recombinant lines for each marker over the total number of lines genotyped is in *italics*. The *dif3* locus was mapped between J22310 and J22700, a 136-kbp region that was sequenced. *B*, structure of the *TIC* gene. The *boxes* represent exons and lines introns. In the predicted structure of *TIC* adapted from Ref. 12, the mutation in *dif3* as in *dif6* was a C-T change in *TIC*, *tic*-2 is a T-DNA insertion mutant, and *tic*-1 an EMS mutant. *C*, expression of *AtFer1* in four *tic* alleles grown on soil. Leaves from 3-week-old plants were collected from each line. The relative transcript level of *AtFer1* was measured by reverse transcriptase Q-PCR, using the *SAND* (A2g28390) housekeeping gene (58) as a control. the values are the means ± S.D. ($n = 3$). *D*, ferritin accumulation in leaves of *dif3*. *E*, ferritin accumulation in leaves of *tic-2*. *D* and *E*, plants were grown as in *C*. Twenty micrograms of total proteins, extracted from leaves, were loaded per lane, and immunodetection was performed using an anti-FER1 serum (17). The *upper panel* shows the autoradiography (*Ferr.*), and the *lower panel* shows the Coomassie Brilliant Blue staining used as a loading control (*Coom.*).

kbp interval between markers J22310 and J22700, localized respectively in the genes At3g22310 and At3g22700 (Fig. 1*A*). This genomic DNA fragment was sequenced, and only one mutation was identified, corresponding to a C-T change leading to a premature stop codon in the tenth exon of the *TIC* gene (At3g22380) (Fig. 1*B*). Another mutant, called *dif6*, was isolated from an independent pool of mutagenized seeds and crossed with *dif3* for an allelism test. The two mutants were shown to be allelic based on the high LUC activity of plants from the F1 progeny (data not shown), suggesting that the mutations in each line affected the same gene. Therefore, the *TIC* gene of *dif6* was sequenced, and a mutation corresponding to a C-T change was identified in the fourth exon of *TIC* (Fig. 1*B*). Two other *tic* alleles were used to confirm the positional cloning of *dif3*: the EMS mutant *tic-1* in Ws background and the T-DNA insertion mutant *tic*-2 in Col background (12, 13) (Fig. 1*B*). Grown on soil, *dif3* and *dif6* exhibited a 10-fold increase in *AtFer1* mRNA abundance compared with transgenic line, *tic-2* exhibited a 16-fold increase compared with Col, and *tic-1* exhibited a 9-fold increase compared with Ws (Fig. 1*C*). Hence, the deregulation of the *AtFer1* gene expression in four independent *tic* alleles confirmed the mapping data. The deregulation observed at the mRNA level also occurred at the protein level because a higher abundance of ferritin proteins was observed in *dif3* (Fig. 1*D*) and in *tic-2* (Fig. 1*E*) compared with the wild type plants. Because *dif3* carried mutations other than the one in the *TIC* gene and because similar results were obtained for the EMS mutant *dif3* and the T-DNA insertion mutant *tic-2*, the latter was used for subsequent experiments.

Phenotypical Characterization of the tic-2 Mutant—We performed some macroscopic and molecular analysis of the *tic-2* mutant to estimate the impact of the mutation on plant growth and development. In a greenhouse, *tic-2* exhibited a strong internerval chlorosis compared with the wild type (Fig. 2*A*). The same chlorosis was observed with the three other mutant alleles (supplemental Fig. S1). This kind of chlorosis was similar to the one observed in the case of iron deficiency (5, 23, 24). When *tic-2* plants were irrigated with iron, the chlorotic phenotype was rescued, indicating that it was due to iron deficiency (Fig. 2*A*). Pigment contents were determined in Col and *tic-2* grown in control conditions. The *tic-2* mutant had a significant decrease of both chlorophyll and carotenoid contents (18 and 22% decrease, respectively; Fig. 2*B*). The iron content in leaves of

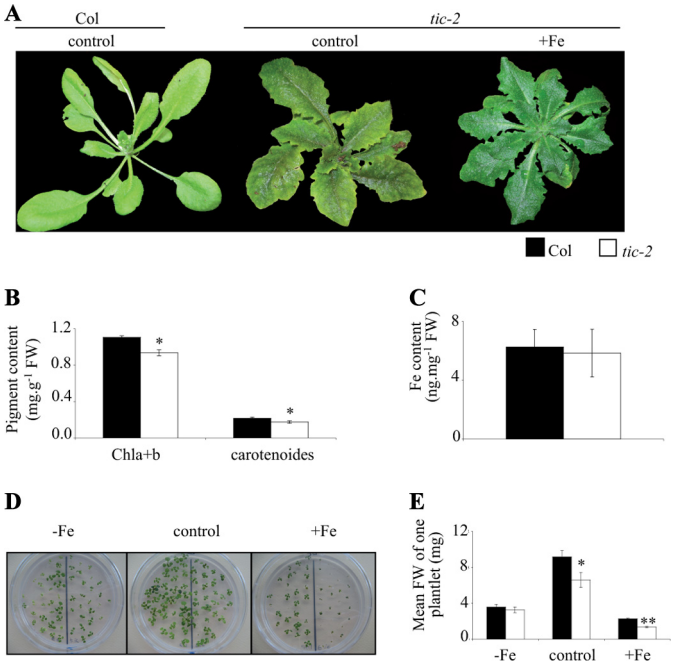

FIGURE 2. **Phenotypical analysis of the *tic-2* mutant in response to iron status.** *A*, representative 4-week-old Col and *tic-2* plants grown on soil in a greenhouse and irrigated with water (*control*) or irrigated with iron-EDDHA 600 μM (+Fe). *B*, determination of pigment content in 4-week-old Col and *tic-2* plants grown on soil in a greenhouse and irrigated with water. *FW*, fresh weight. *C*, determination of iron content in the leaves of 4-week-old Col and *tic-2* plants grown on soil in a greenhouse and irrigated with water. Shown are the means ± S.D. of nine measurements (three replicates/experiment performed three times). *D*, iron sensitivity of plants grown as followed. The plants were grown *in vitro* during 2 weeks on medium without the addition of iron (−*Fe*), with the addition of iron-EDTA 50 μM (control), or with the addition of Fe- EDTA 500 μM (+*Fe*). Col is on the *left half* of each panel, and *tic-2* on the *right half*. *E*, mean fresh weight of one plantlet. The plants were grown as described for *D*. The weight of a plantlet was calculated as followed: weight of a plantlet = (fresh weight of plantlets of a genotype from the same plate)/(number of plantlets of a genotype from the same plate). *B* and *E*, shown are the means ± S.D. ($n = 3$). *B*, *C*, and *E*, *, $p < 0.05$; **, $p < 0.01$; *black* and *white bars* represent, respectively, Col and *tic-2*.

Col and *tic-2* was similar (Fig. 2*C*), indicating that the chlorotic phenotype observed for *tic-2* was not due to an iron uptake or translocation from roots to shoots defect. Because the mutant seemed to be sensitive to iron supply on soil, its early development was analyzed in various iron nutrition conditions: deficiency (0 μM iron-EDTA, −*Fe*), sufficiency (50 μM iron-EDTA, *control*), and excess (500 μM iron-EDTA, +*Fe*). Grown *in vitro*, *tic-2* development was affected on both iron-sufficient and iron excess media, but not on iron-deficient medium (Fig. 2*D*). Except under iron deficiency, *tic-2* plantlets were smaller revealing sensitivity to iron. The production of fresh weight of Col and *tic-2* plantlets was measured. On control and +Fe media, *tic-2* biomass was, respectively, 30 and 40% lower than Col (Fig. 2*E*). This whole set of results showed that a mutation in the *TIC* gene led to alterations in iron homeostasis and to sensitivity to iron excess.

TIC-mediated AtFer1 Regulation Is Circadian Clock-dependent—The *TIC* gene encodes a nuclear regulator of the circadian clock (12). Thus, a potential TIC-mediated regulation of *AtFer1* expression through the circadian clock was investigated. Col plants were grown on soil in light/dark (LD) conditions then transferred in free running conditions *i.e.* in continuous light (LL) to discriminate between circadian and diurnal regulations. The persistence of rhythmic expression in such a condition is the signature of a clock-controlled gene. *LHY* (late elongated hypocotyl) (25, 26) was used as a control of circadian-controlled genes. *LHY* and *AtFer1* mRNA accumulations were monitored every 4 h at the indicated Zeitgeber times for 48 h (Fig. 3, *A* and *B*). As expected, *LHY* mRNA accumulation presented exactly the same 24-h rhythm in LD and LL conditions (Fig. 3*A*). *AtFer1* mRNA accumulation was rhythmic under LD conditions with a 24-h period (Fig. 3*B*) and peaked 3 h after dawn with a distinct phase of *LHY*, which peaked 1 h before dawn (Fig. 3*A*). Surprisingly, under free running conditions of continuous light, *AtFer1* expression exhibited an 8-h phase advance compared with LD (Fig. 3*B*) and seemed to remain rhythmic at least during the first cycle. This suggested that *AtFer1* expression could be controlled by the clock and responds to light changes with a high mRNA accumulation at dawn.

To confirm this hypothesis, mutants in the central oscillator of the circadian clock were used to analyze the *AtFer1* expression in a clock breakdown background. The mutants impaired in the central oscillator used for the experiment were *elf4-1* (27), *lhy-21* (26), and *cca1-11* (28), the insertion of the two latest being remapped (supplemental Fig. S2). *ELF4* (early flowering 4) is one component of the evening loop of the oscillator (29), and the *elf4-1* mutant showed a reduced capacity to anticipate dawn (30), making it relevant because *AtFer1* expression is induced by dawn. *LHY* and *CCA1* (circadian clock-associated 1) are components of the morning loop of the oscillator (29), allowing us to analyze *AtFer1* response in both loops. The wild type parental line, Ws, displayed the same rhythmic *AtFer1* expression as Col, whereas *elf4-1*, *lhy-21* and *cca1-11* did not lay out any rhythm in *AtFer1* mRNA accumulation (Fig. 3*C*). Finally, we investigated the involvement of TIC, described as an upstream regulator of the central oscillator (12, 31), on *AtFer1* expression for 48 h in plants grown in LD conditions (Fig. 3*D*). The *AtFer1* mRNA level was higher in *tic-2* compared with Col at each Zeitgeber time point (Fig. 3*D*), which is consistent with the up-regulation observed in the genetic screen. *AtFer1* expression appeared arrhythmic in *tic-2*, a result expected for the effect of a component of the circadian clock on an output target (31, 32). Taken together, these results suggested that *AtFer1* expression is regulated by the circadian clock through a *TIC*-dependent pathway.

Mutation in the TIME FOR COFFEE Gene Affects Iron Homeostasis in Arabidopsis—AtFer1 has been reported to be regulated by iron (9, 33); we thus investigated whether TIC is involved in the iron-dependent *AtFer1* expression and more generally whether other iron-regulated genes could be regulated by TIC. *AtFer1* expression was investigated in the *tic-2* mutant in response to iron supply. The analysis was performed on leaves where *AtFer1* is mainly expressed (8, 34). The expression of *AtFer1* was analyzed on hydroponically grown plants with two iron supply conditions (iron deficiency and iron overload after deficiency). In iron-starved plants (−*Fe*) and in plants treated with iron citrate 500 μM for 5 h (+*Fe*), the expression of *AtFer1* was higher in *tic-2* than in Col (Fig. 4*A*). The fold of *AtFer1* mRNA accumulation in response to iron was ~150 in

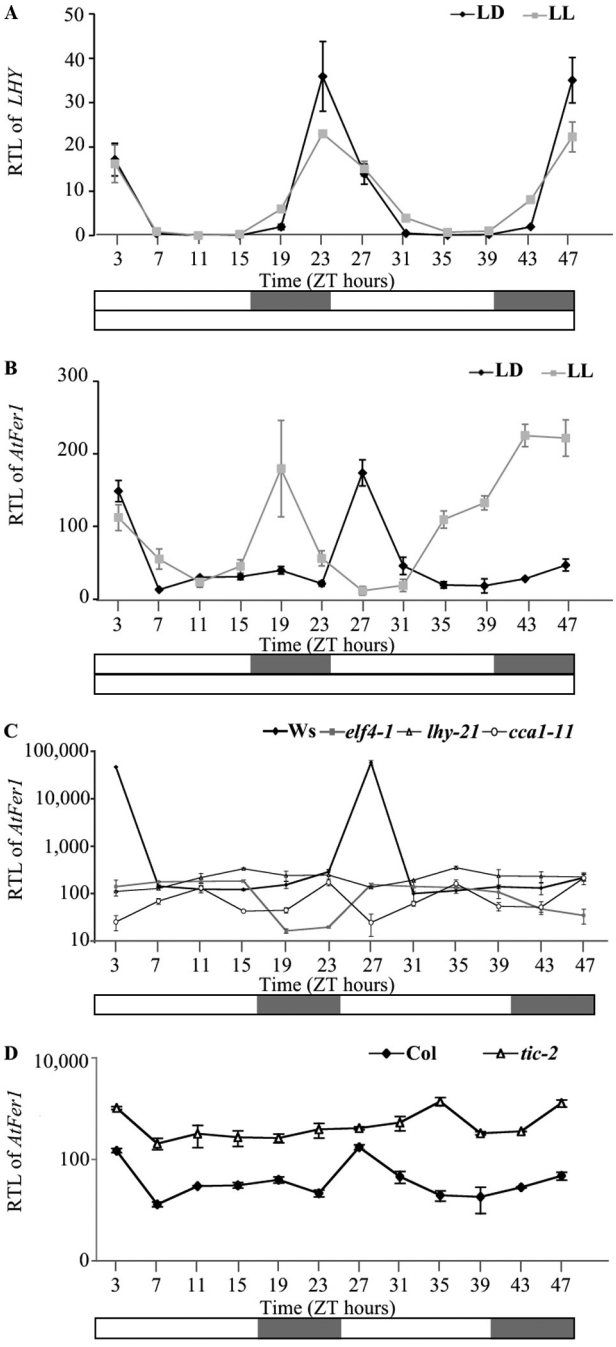

FIGURE 3. **Release experiments for analyzing the *AtFer1* regulation.** The plants were grown on soil under 16 h of light/8 h of dark (LD) cycles. Two-week-old plantlets were then transferred into LL or kept under LD cycles before harvesting leaves every 4 h for 2 days. RTLs were assayed by Q-PCR relatively to an internal *EF1α* control (At1g07930). *A*, RTL of *LHY* in Col plants under LD and LL conditions. *B*, RTL of *AtFer1* in Col plants under LD and LL conditions. *Black diamonds* and *gray squares* represent, respectively, LD and LL (*A* and *B*). *C*, RTL of *AtFer1* in Ws, *elf4-1*, *lhy-21*, and *cca1-11* plants under LD conditions. *Black diamonds*, *gray squares*, *open triangles*, and *open circles* represent, respectively, Ws, *elf4-1*, *lhy-21*, and *cca1-11*. *D*, RTL of *AtFer1* in Col and *tic-2* plants under LD conditions. *Black diamonds* and *open triangles* represent, respectively, Col and *tic-2*. *A–D*, shown are the means ± S.D. ($n = 3$); *open bars* indicate light intervals, and *closed bars* indicate dark intervals; *ZT*, Zeitgeber time.

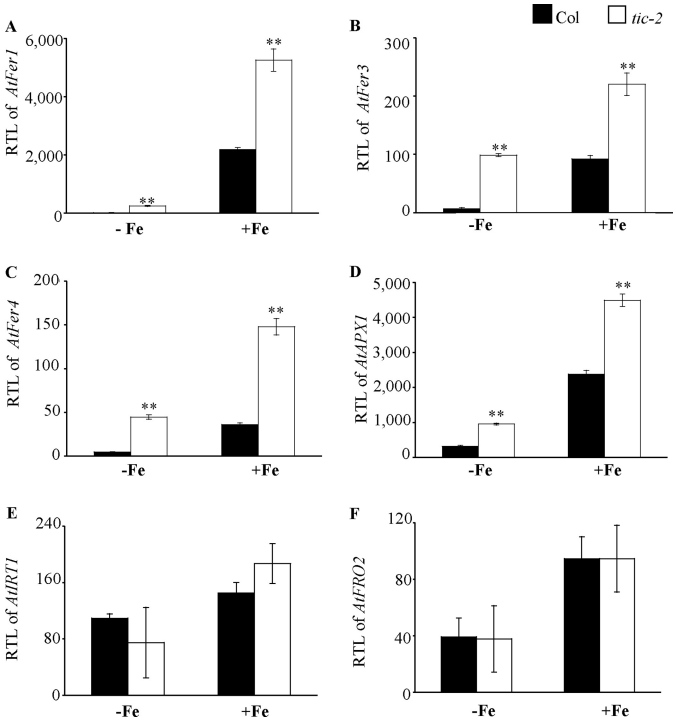

FIGURE 4. **Expression of iron-responsive genes in *tic-2*.** Six-week-old plants, grown in hydroponic condition under iron sufficiency, were submitted to different iron treatments: iron deficiency during 1 week (−*Fe*) and iron overload for 5 h after 1 week of deficiency (+*Fe*). The leaves and roots were harvested separately, and RTL were measured by Q-PCR using *PP2* (At1g13320), as a housekeeping gene (58). *A*, RTL of *AtFer1* in leaves under iron deficiency and overload. *B*, RTL of *AtFer3* in leaves under iron deficiency and overload. *C*, RTL of *AtFer4* in leaves under iron deficiency and overload. *D*, RTL of *AtAPX1* in leaves under iron deficiency and overload. *E*, RTL of *AtIRT1* in roots under iron deficiency and overload. *F*, RTL of *AtFRO2* in roots under iron deficiency and overload. *Black* and *white bars* represent, respectively, Col and *tic-2*; shown are the means ± S.D. ($n = 3$); **, $p < 0.01$ (*A–D*).

Col and ~20 in *tic-2*. Thus, the *AtFer1* mRNA abundance was still increased in response to iron excess in *tic-2*, and the smaller fold of increase in *tic-2* seemed to be more related to a higher basal level in iron deficiency than to a defect in iron overload responsiveness. Under iron deficiency, *AtFer1* expression was 17-fold higher in *tic-2* than in Col. After iron overload, it was only 2.4-fold higher, suggesting that the TIC effect on *AtFer1* expression was strongest under iron deficiency. This allowed us to conclude that TIC is necessary to repress *AtFer1* gene expression under iron deficiency. Its impact appears to be the strongest under iron-deficient conditions at the molecular level, whereas the chlorotic phenotype was observable under iron sufficiency (Fig. 2*A*). Moreover, TIC is not involved in the iron responsiveness of *AtFer1*.

Like *AtFer1*, the *AtFer3* and *AtFer4* ferritin genes and the cytosolic ascorbate peroxidase *AtAPX1* are also expressed in vegetative tissues, and their transcript abundance is increased in response to iron overload (8, 34, 35). We thus investigated whether the mutation in the *TIC* gene altered *AtFer3*, *AtFer4*, and *AtAPX1* expression in leaves of plants grown under the same conditions as described above. The mRNA levels of these three genes were higher in *tic-2* compared with Col in both iron nutrition conditions (Fig. 4, *B–D*). As observed for *AtFer1*, the fold of accumulation of these three transcripts in response to iron was lower because the level of mRNA accumulation was higher under iron starvation in *tic-2*. We next investigated whether the deregulation of these genes was directly related to the mutation in *TIC*, as for *AtFer1*, or indirectly resulting from a TIC-dependent increase of *AtFer1* mRNA accumulation.

Indeed, it was shown that the alteration of ferritin genes expression could impact the expression of other genes involved in iron homeostasis (8). For discriminating between these two hypotheses, a transgenic line overexpressing *AtFer1* under the control of the 35S promoter (p^{35S}::*AtFer1*) was used (supplemental Fig. S3*A*) and grown in the same conditions as above. The mRNA levels of *AtFer3*, *AtFer4*, and *AtAPX1* were not affected in the overexpressing line, whatever the iron supply (supplemental Fig. S3, *B–D*). Thus, the overexpression of *AtFer1* did not lead to the modulation of *AtFer3*, *AtFer4*, and *AtAPX1* expression. This result indicated that TIC is necessary to keep *AtFer3*, *AtFer4*, and *AtAPX1* gene expression at a low level under iron deficiency.

Because the effect of the *tic-2* mutation was more obvious under iron deficiency and because *tic-2* was chlorotic on soil, the expression of genes up-regulated in response to iron starvation was analyzed in the roots of wild type and *tic-2* plants grown in the same conditions as described above. The *AtIRT1* (iron(II) responsive transporter 1) (36) and *AtFRO2* (ferric-chelate reductase oxidase 2) (37) genes were selected. In contrast to the iron excess-responsive genes analyzed, no significant difference in *AtIRT1* (Fig. 4*E*) and *AtFRO2* (Fig. 4*F*) mRNA accumulation was observed between wild type and *tic-2* roots, regardless of the iron status. Thus, TIC has no impact on iron deficiency-regulated genes encoding the root iron uptake system, such as *AtIRT1* and *AtFRO2*. By contrast, TIC represses the expression of iron overload-regulated genes, such as ferritins, under low iron conditions. Put together, these data showed that TIC is required for proper iron homeostasis in *Arabidopsis*.

TIC-mediated AtFer1 Regulation Is IDRS-independent—The data described above indicated that TIC acts in the repressive pathway leading to a low *AtFer1* expression under iron deficiency (Fig. 4*A*). TIC regulates *AtFer1* expression under repressive conditions through the circadian clock (Fig. 3). The IDRS box located in the *AtFer1* promoter is a *cis*-acting element involved in the repression of *AtFer1* transcription under iron deficiency (9). Consequently, we investigated whether the TIC-mediated *AtFer1* regulation occurs through the IDRS. Two transgenic lines in Col background were used (9): *At1400IDRS*::*GUS* (named p*IDRS*::GUS Col) and *At1400m*IDRS*::*GUS* (named p*IDRS**::*GUS* Col) carrying 1.4 kbp of the *AtFer1* promoter region with, respectively, a wild type and a mutated IDRS sequence, fused to the GUS reporter gene. The two lines were crossed with *tic-2*, and homozygous lines for both loci were selected in the F2 progeny. They were named p*IDRS*::*GUS tic-2* and p*IDRS**::*GUS tic-2*. Seedlings of each line were grown *in vitro* for 10 days on iron-sufficient medium (50 μM iron-EDTA) and then transferred on an iron-depleted medium containing ferrozine 200 μM (−*Fe*) for 4 days. Afterward, half of the iron-starved plants were treated with 500 μM iron citrate for 5 h for iron overload treatment (+*Fe*). Both treatments were controlled by analyzing, respectively, the induction of *AtIRT1* in iron-starved roots and of *AtFer1* in iron-overloaded leaves (data not shown).

The transcript abundance of the *GUS* reporter gene was determined in leaves of the four transgenic lines (Fig. 5). As expected, the *GUS* mRNA abundance was higher in the

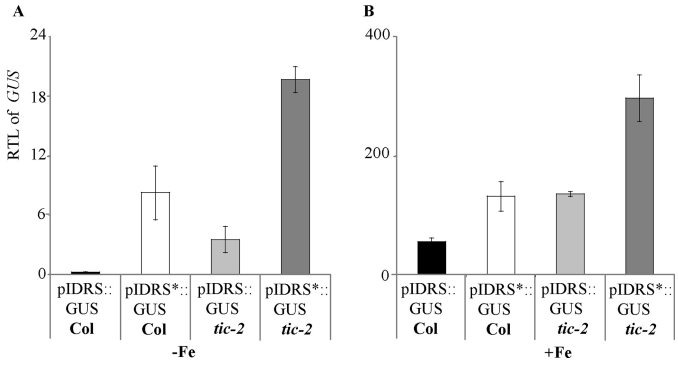

FIGURE 5. **Involvement of TIC and the IDRS *cis*-element in the *AtFer1* regulation.** The *tic-2* mutant was crossed with the transgenic lines p*IDRS*::*GUS* Col and p*IDRS**::*GUS* Col to produce the lines p*IDRS*::*GUS tic-2* and p*IDRS**::*GUS tic-2*. The plants were grown *in vitro* under iron sufficiency during 10 days before being transferred for 4 days on iron-starved medium (−*Fe*). For the iron excess treatment, part of the iron-starved plants was sprayed with iron citrate 500 μM (+*Fe*). Leaves from plants grown on the different iron conditions were collected 5 h after the iron spray. The *GUS* RTL was measured in leaves by Q-PCR, using *PP2* (At1g13320) as a housekeeping gene (58). *A*, RTL of the *GUS* reporter gene in iron deficiency. *B*, RTL of the *GUS* reporter gene in response to iron excess. Shown are the means ± S.D. with $n = 3$ (*A* and *B*).

p*IDRS**::*GUS* Col and p*IDRS*::*GUS tic-2* lines than in the p*IDRS*::*GUS* Col in both iron conditions (Fig. 5). On both iron nutrition conditions, the *GUS* mRNA accumulation was significantly higher in the p*IDRS**::*GUS tic-2* line than in the p*IDRS**::*GUS* Col and p*IDRS*::*GUS tic-2* lines. Moreover, the sum of the *GUS* RTL values for the p*IDRS**::*GUS* Col and p*IDRS*::*GUS tic-2* lines was almost equal to the RTL value for the p*IDRS**::*GUS tic-2* line. These data indicated that the *tic-2* mutation and the IDRS mutated *cis*-element have independent and additive effects on the *GUS* mRNA abundance. Thus, it appears that *AtFer1* is transcriptionally repressed by two independent pathways, one involving the *cis*-element IDRS and the other one involving the *TIC* gene.

TIC Requires LD Cycles and Light to Regulate AtFer1 Expression—*AtFer1* was reported to be up-regulated during dark-induced senescence (10). Because TIC seems to transduce the light signal to the central oscillator of the circadian clock and because *AtFer1* expression responds to dawn or lighting by a huge increase in transcript accumulation (Fig. 3*B*), we wanted to determine whether the dark-induced *AtFer1* expression depended on TIC, whether the effect of the *tic-2* mutation was still effective in darkness, and finally whether the TIC-mediated regulation of *AtFer1* expression required light. Col and *tic*-2 plants were grown on soil in LD conditions for 2 weeks. They were then maintained in LD conditions (Fig. 6, *A* and *B*) or transferred in continuous darkness for 3 days (Fig. 6, *C* and *D*). The samples were collected 30 min before dawn (T_0) and then 24 h (T_1), 48 h (T_2), or 72 h (T_3) later. After these 3 days, the light was switched on, and the samples were collected 1, 3, and 5 h after lighting.

Under LD conditions, in *tic-2*, the accumulation of *AtFer1* mRNA and of ferritin protein were systematically higher at dawn (Fig. 6, *A* and *B*), and *AtFer1* mRNA was strongly over-accumulated in response to light (Fig. 6*A*). When plants were maintained in dark, *AtFer1* mRNA and ferritin protein were highly accumulated in Col, as expected for a dark-induced

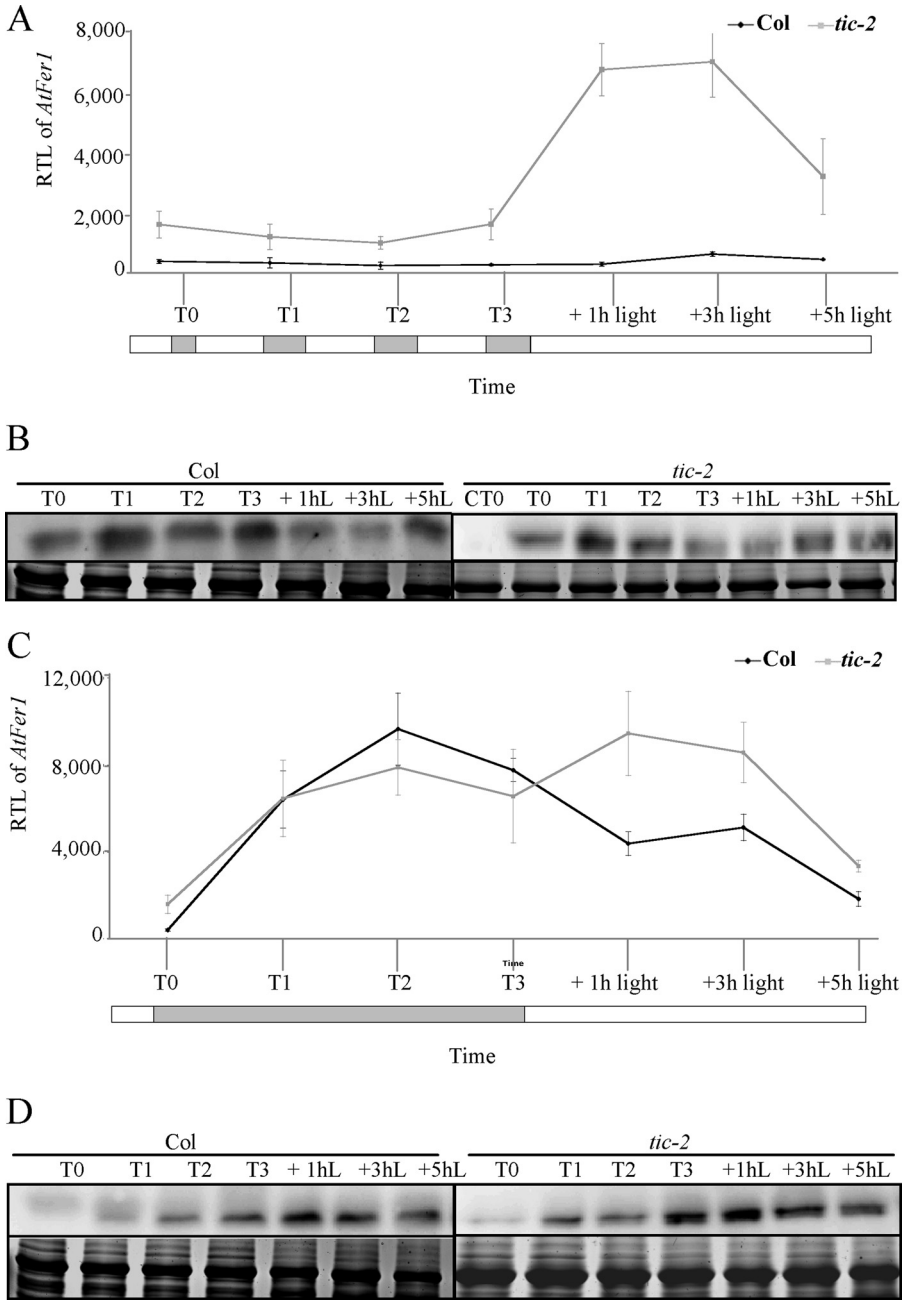

FIGURE 6. **Dark-induced *AtFer1* expression and response to a light return.** Col and *tic-2* plants were grown on soil under 16 h of light/8 h of dark cycles for 2 weeks. The 15th day, 30 min before lighting (T_0), leaves of Col and *tic-2* plants were collected afterward the remaining plants were kept in the same condition (LD) or transferred into continuous darkness. Triplicate samples were harvested every 24 h for 3 days (T_1, T_2, and T_3). The third day, at the subjective dawn, the plants were turned back in light, and triplicate samples were harvested 1, 3, and 5 h after transfer. *A*, RTL of *AtFer1* in LD. *B*, ferritin accumulation in LD; *CT0*, Col at T_0. *C*, RTL of *AtFer1* in continuous darkness. *D*, ferritin accumulation in continuous darkness. RTLs of *AtFer1* were assayed by Q-PCR relatively to an internal *EF1*α control (At1g07930); shown are the means ± S.D. ($n = 3$); *open* and *closed bars* indicate, respectively, light and dark intervals (*A* and *C*). Ferritin accumulation was assayed by Western blot; 20 μg of total proteins, extracted from leaves, were loaded per lane, and immunodetection was performed using an anti-FER1 serum (16). The *upper panel* is the autoradiography (*Ferr.*), and the *lower panel* is the Coomassie Brilliant Blue staining used as a loading control (*Coom.*); *hL*, h of light treatment (*B* and *D*).

gene. However, this accumulation was the same in *tic-2* when compared with Col, suggesting that the TIC effect on *AtFer1* expression was abolished by continuous darkness (Fig. 6*C*). The high accumulation of ferritin in response to continuous darkness also occurred at the protein level in *tic-2* but slightly more quickly when compared with Col (Fig. 6*D*). When light was switched on after the 3 days of dark, *AtFer1* transcript was slightly overaccumulated in *tic-2*, but not in Col, suggesting that light is required for TIC-repressive activity. Taken together, these results indicated that TIC is not involved in the dark-induced *AtFer1* expression and that both LD cycles and light are required for the TIC repression of *AtFer1* expression.

DISCUSSION

A LUC-based genetic screen using the *AtFer1* iron-responsive promoter was initiated to identify regulators of iron homeostasis. This genetic screen led to the identification of TIME FOR COFFE as a new regulator of the *AtFer1* gene expression. We investigated the function of TIC and of the central oscillator of the circadian clock on the expression of *AtFer1* and of other iron overload-responsive genes. We showed that iron overload-expressed genes are regulated by TIC and by the central oscillator of the circadian clock. TIC represses their expression under low iron conditions, and its activity requires light and LD cycles. For *AtFer1*, this repression is independent of the previously characterized *cis*-acting element IDRS, known to be involved in *AtFer1* repression. Finally, mutants in the *TIC* gene exhibited a chlorotic phenotype rescued by exogenous iron addition and are hypersensitive to iron during the early stages of development. These results showed that the regulation of iron homeostasis in plants is a major output of TIC-dependent and central oscillator-dependent signaling pathways.

TIC-, Circadian Clock-, and Light-mediated AtFer1 Regulation—The circadian clock generates endogenous 24-h rhythms and allows the anticipation of light and temperature changes in plants (31, 38). TIC was previously described as a nuclear regulator of the circadian clock in *Arabidopsis* and is specific to plants (12, 13). Because TIC is involved in a circadian network, we first investigated whether the TIC-mediated *AtFer1* regulation occurs through a circadian mechanism. Our

data showed that *AtFer1* mRNA accumulation follows a 24-h rhythm in LD conditions (Fig. 3*B*). Surprisingly, in LL conditions, *AtFer1* mRNA accumulation showed a 8-h phase advance compared with LD (19 h Zeitgeber time instead of 27 h Zeitgeber time) (Fig. 3*B*). It was previously shown that *CAB* expression peaked 6 h earlier in *tic-1* than in the wild type and that the oscillator was arrested in this mutant after 19 h of light (13). The use of mutants impaired in the morning (*lhy-21* and *cca1-11*) and in the evening (*elf4-1*) loops of the central oscillator confirmed that the TIC-mediated *AtFer1* expression occurs through the clock, because *AtFer1* mRNA accumulation was not rhythmic in these mutants under LD conditions (Fig. 3*D*). Put together, these results suggested that TIC regulates *AtFer1* expression through a circadian pathway.

The rhythm of *AtFer1* mRNA accumulation was lost in *tic-2*, and the transcript amount was systematically higher when compared with Col (Fig. 3*D*). This result showed that TIC represses *AtFer1* expression in low iron condition and that the repressed state of *AtFer1* is clock-regulated. The IDRS *cis*-element, located in the proximal region of the *AtFer1* promoter, has already been shown to be involved in *AtFer1* repression (9). A regulating pathway involving the *trans*-element TIC and the *cis*-element IDRS was therefore an attractive hypothesis to test. The analysis of *Arabidopsis* transgenic lines, carrying either a mutation in the *TIC* gene and/or in the IDRS, demonstrated that the effects of both mutations were additive and, thus, that the TIC-mediated *AtFer1* regulation is independent of the IDRS (Fig. 5). It has been reported that, when plants carrying a p*IDRS*::*GUS* construct were subjected to a prolonged dark treatment, an increase of GUS activity was observed and that this phenomenon is IDRS-dependent (10). In our study, *AtFer1* transcript accumulation and ferritin protein accumulation occurred similarly in Col and *tic-2* exposed to prolonged darkness (Fig. 6, *C* and *D*), showing that the dark-induced expression of *AtFer1* is independent of the TIC regulator, which is consistent with the IDRS independence of the TIC-mediated *AtFer1* regulation (Fig. 5). Thus, *AtFer1* expression is under the control of two independent repressive pathways: one involving the IDRS *cis*-element and controlling the dark-induced transcriptional activation and one involving TIC and controlling the circadian-dependent *AtFer1* regulation.

AtFer1 expression is rhythmic, and the transcript amount peaks at dawn (Fig. 3*B*). Dawn is a time favorable for light-induced oxidative stress in leaves, and ferritins were shown to be involved in the protection against oxidative stress (8). Thus, it was consistent that the maximum level of *AtFer1* mRNA abundance was observed at this time. We showed that the TIC-mediated *AtFer1* regulation requires light and LD cycles (Fig. 6). TIC and ELF3 were reported to transduce the light signal to the central oscillator and to affect the circadian clock *via* the gating mechanism (12, 13, 39–41). The *tic* and the *elf3* mutations seem to show an epistatic interaction, and phenotypes in the double mutant *tic elf3* were additive or intermediate between the single mutants (12, 13). Thus, it should be interesting to analyze *AtFer1* expression in *elf3* and *tic elf3* mutants to determine whether the rhythm and the dawn-induced transcript accumulation are affected. This will allow us to know whether ELF3, like TIC, is necessary for the regulation of *AtFer1* expression, and whether they act redundantly.

TIC Controls Iron Homeostasis—Most of the studies regarding the regulation of ferritin expression focused on the transcriptional activation by iron (reviewed in Ref. 42). Thus, we investigated whether a link between the TIC-mediated regulation and the iron-signaling pathway exists, especially if TIC could affect other iron-responsive gene expression (Fig. 4). Indeed, *AtFer3*, *AtFer4*, and *AtAPX1* expression was up-regulated in *tic-2*. The analysis of an *AtFer1* overexpressing line clearly demonstrated that the increase of *AtFer3, AtFer4*, and *AtAPX1* mRNA levels in *tic-2* was not a secondary effect of the *AtFer1* overexpression but resulted from the *tic* mutation itself. Consequently, besides *AtFer1*, TIC is also a repressor of *AtFer3*, *AtFer4*, and *AtAPX1* expression. Interestingly, in contrast to *AtFer1*, which is derepressed by iron through the IDRS box (9), *AtAPX1* is transcriptionally activated by iron (35). Thus, TIC acts as a repressor of both iron derepressed, *i.e. AtFer1*, and iron activated, *i.e. AtAPX1*, genes. By contrast, TIC did not affect the expression of iron deficiency-regulated genes such as *AtIRT1* or *AtFRO2*, and that was independent of the iron supply conditions (Fig. 4, *E* and *F*). Interestingly, whereas ferritin overexpression increases root ferric reductase activity and leaf iron concentration in tobacco plants (43), the root iron uptake system was not activated in *tic-2*. This result suggested that overexpression of ferritin protein and a high ferritin gene expression arising from a TIC-mediated regulation defect did not lead to the same effect on the root iron uptake system.

Analysis of the *tic-2* mutant showed that the mutation in the *TIC* gene led to phenotypes related to iron (Fig. 2). When grown on soil, *tic-2* exhibited an iron chlorosis, but because the total iron content was not changed in the mutant, this suggested that *tic-2* was plausibly affected in iron use or location at the cellular or at the subcellular level rather than in iron uptake or translocation from roots to shoots (Fig. 4) (44). When grown *in vitro*, *tic-2* plantlets were affected in their early development on both iron-sufficient or excess media. Thus, TIC appears to be a central regulator of iron homeostasis in plants. This study made, for the first time, the link between the iron nutrition and the circadian clock and showed that the control of iron homeostasis appears to be a new output of the light/circadian clock pathways. In arable soil, iron is poorly available for plants (45), and iron starvation is commonly encountered. Iron is a limiting factor for plant productivity and biomass production (8, 46, 47). Thus, plants do probably not often experience iron overload. Therefore, in natural conditions where iron is poorly available, light, circadian clock, and TIC are likely to constitute the major signaling pathway of iron homeostasis regulation.

The next challenge will be to identify additional factors and components in this pathway, with special emphasis on the elements specific for the regulation of iron homeostasis. TIC is constitutively present among the circadian time (12), and *AtFer1* expression is not all the time repressed by TIC. This raises the question of the regulation of TIC activity during circadian time. A putative P-loop motif, common to numbers of ATP/GTP-binding proteins, was identified in the TIC protein (12). It was suggested that this P-loop could bind to and be phosphorylated by a protein kinase (12). TIC activity could be

regulated by (de)phosphorylation events (12), and interestingly, a PP2A-type phosphatase promotes an increase of *AtFer1* mRNA level (33). Hence, TIC could regulate *AtFer1* expression according to its phosphorylation state. The phosphorylated form could repress *AtFer1* expression all the time, except at dawn when the unphosphorylated form would allow the increase of *AtFer1* expression.

Recently, the Davis group screened for interactors of TIC and isolated the SNF1 stress-related kinase AKIN10 (48). AKIN10 is homologous to two members of the conserved energy sensor protein kinase family, SNF1 (sucrose nonfermenting 1) in yeast and AMPK (AMP-activated protein kinase) in mammals, and was proposed as a master metabolic sensor (49, 50). The SnRK1 (Snf1-related kinase) members AKIN10 and its homologue AKIN11 were shown to interact with SKP1/ASK1 (S phase kinase-associated protein 1/*Arabidopsis* SKP1-like 1) that mediates proteasomal binding of an ubiquitin ligase (51). This interaction is inhibited by PRL1 (pleiotropic response locus 1) that seemed to compete with SKP1 for binding to the C-terminal regulatory domain of AKIN10 and AKIN11. A recent genetic screen for identifying genes involved in the singlet oxygen signaling pathway (52) led to the isolation of a mutant in the *PRL1* gene. Interestingly, the characterization of the *prl1-5* mutant showed that the expression of *AtFer1* and *AtAPX1* was constitutively repressed in this mutant when compared with Col (53). This result suggested that PRL1 could be a positive regulator of the TIC activity. Thus, a regulatory network involving TIC, AKIN10, and PRL1 could be hypothesized for regulating iron homeostasis. TIC would be active when phosphorylated and would repress the *AtFer* and *AtAPX1* genes. This active state would be (directly or indirectly) promoted by the AKIN10 kinase, and dawn favors the dephosphorylation of TIC, leading to the activation of the target gene expression. Because AKIN10 is negatively regulated by PRL1, AKIN10 could so constitutively activate TIC in *prl1* mutants, leading to a lack of *AtFer* and *AtAPX1* derepression at dawn and to a constitutive repression (53).

Input Signal Integration—Our study identified TIC as a major regulator of iron homeostasis in plants. Interestingly, two integrators of stress and energy signaling, AKIN10 (49) and PRL1 (53, 54), were recently shown to be connected to TIC and/or involved in the regulation of some iron-responsive gene expression. In response to energy deficit associated with stresses, the SnRK1 kinases seem to initiate genome-wide transcriptional changes that allow to restore homeostasis and to develop long term responses contributing to adaptation and preservation of growth and development. Regulatory mechanisms were evidenced to coordinate several inputs, such as light, circadian clock, or nutrient signals, into a complex signaling network in which only some insights have started to be understood (49, 55–57). Considering the essential functions of iron and iron-containing proteins in central metabolic processes such as photosynthesis, respiration, nitrogen, and sulfur assimilation (reviewed in Ref. 42), interplays regulating iron homeostasis should be assessed and elucidated to understand how the cellular energy signaling is fully integrated into whole plant adaptation and regulation of growth and development.

Acknowledgments—We thank Seth J. Davis (Max Planck Institute for Plant Breeding Research, Cologne, Germany) for the gift of tic-1, tic-2, and elf4-1 seeds and Cécile Lambert for technical assistance in the map-based cloning. We thank the Salk Institute Genomic Analysis Laboratory (SIGNAL) for providing the sequence-indexed Arabidopsis T-DNA insertion mutants and the Nottingham Arabidopsis Stock Centre for providing seeds.

REFERENCES

1. Cadenas, E. (1989) *Annu. Rev. Biochem.* **58,** 79–110
2. Andrews, N. C. (2000) *Nat. Rev. Genet.* **1,** 208–217
3. Andrews, S. C., Robinson, A. K., and Rodriguez-Quinones, F. (2003) *FEMS Microbiology Reviews* **27,** 215–237
4. Kim, S. A., and Guerinot, M. L. (2007) *FEBS Lett.* **581,** 2273–2280
5. Briat, J. F., Curie, C., and Gaymard, F. (2007) *Curr. Opin. Plant. Biol.* **10,** 276–282
6. Briat, J., Cellier, F., and Gaymard, F. (2005) Ferritins and iron accumulation in plant tissues. In *Iron Nutrition in Plants and Rhizospheric Microorganisms* (Barton, L., and Abadia, J. eds.), Kluwer Academic
7. Pilon, M., Cohu, C. M., Ravet, K., Abdel-Ghany, S. E., and Gaymard, F. (2009) *Curr. Opin. Plant. Biol.* **12,** 347–357
8. Ravet, K., Touraine, B., Boucherez, J., Briat, J. F., Gaymard, F., and Cellier, F. (2009) *Plant J.* **57,** 400–412
9. Petit, J. M., van Wuytswinkel, O., Briat, J. F., and Lobréaux, S. (2001) *J. Biol. Chem.* **276,** 5584–5590
10. Tarantino, D., Petit, J. M., Lobréaux, S., Briat, J. F., Soave, C., and Murgia, I. (2003) *Planta* **217,** 709–716
11. Patton, E. E., Willems, A. R., and Tyers, M. (1998) *Trends Genet.* **14,** 236–243
12. Ding, Z., Millar, A. J., Davis, A. M., and Davis, S. J. (2007) *Plant Cell* **19,** 1522–1536
13. Hall, A., Bastow, R. M., Davis, S. J., Hanano, S., McWatters, H. G., Hibberd, V., Doyle, M. R., Sung, S., Halliday, K. J., Amasino, R. M., and Millar, A. J. (2003) *Plant Cell* **15,** 2719–2729
14. Lobréaux, S., Thoiron, S., and Briat, J. (1995) *Plant J.* **8,** 443–449
15. Clough, S. J., and Bent, A. F. (1998) *Plant J.* **16,** 735–743
16. Liu, Y. G., Mitsukawa, N., Oosumi, T., and Whittier, R. F. (1995) *Plant J.* **8,** 457–463
17. Dellagi, A., Rigault, M., Segond, D., Roux, C., Kraepiel, Y., Cellier, F., Briat, J. F., Gaymard, F., and Expert, D. (2005) *Plant J.* **43,** 262–272
18. Schaffner, W., and Weissmann, C. (1973) *Anal. Biochem.* **56,** 502–514
19. Laemmli, U. (1970) *Nature* **227,** 680–685
20. MacKinney, G. (1941) *J. Biol. Chem.* **140,** 315–322
21. Lobréaux, S., and Briat, J. (1991) *Biochem. J.* **274,** 601–606
22. Beinert, H. (1978) *Methods Enzymol.* **54,** 435–445
23. Briat, J. F., Fobis-Loisy, I., Grignon, N., Lobréaux, S., Pascal, N., Savino, G., Thoiron, S., von Wiren, N., and Van Wuytswinkel, O. (1995) *Biol. Cell* **84,** 69–81
24. Curie, C., and Briat, J. F. (2003) *Annu. Rev. Plant. Biol.* **54,** 183–206
25. Carré, I. A., and Kim, J. Y. (2002) *J. Exp. Bot.* **53,** 1551–1557
26. Schaffer, R., Ramsay, N., Samach, A., Corden, S., Putterill, J., Carré, I. A., and Coupland, G. (1998) *Cell* **93,** 1219–1229
27. Doyle, M. R., Davis, S. J., Bastow, R. M., McWatters, H. G., Kozma-Bognar, L., Nagy, F., Millar, A. J., and Amasino, R. M. (2002) *Nature* **419,** 74–77
28. Wang, Z. Y., and Tobin, E. M. (1998) *Cell* **93,** 1207–1217
29. Mas, P. (2008) *Trends Cell Biol.* **18,** 273–281
30. McWatters, H. G., Kolmos, E., Hall, A., Doyle, M. R., Amasino, R. M., Gyula, P., Nagy, F., Millar, A. J., and Davis, S. J. (2007) *Plant Physiol.* **144,** 391–401
31. Mas, P. (2005) *Int. J. Dev. Biol.* **49,** 491–500
32. Somers, D. E., Webb, A. A., Pearson, M., and Kay, S. A. (1998) *Development* **125,** 485–494
33. Arnaud, N., Murgia, I., Boucherez, J., Briat, J. F., Cellier, F., and Gaymard, F. (2006) *J. Biol. Chem.* **281,** 23579–23588
34. Petit, J. M., Briat, J. F., and Lobréaux, S. (2001) *Biochem. J.* **359,** 575–582

35. Fourcroy, P., Vansuyt, G., Kushnir, S., Inze, D., and Briat, J. F. (2004) *Plant Physiol.* **134,** 605–613
36. Vert, G., Grotz, N., Dedaldechamp, F., Gaymard, F., Guerinot, M. L., Briat, J. F., and Curie, C. (2002) *Plant Cell* **14,** 1223–1233
37. Robinson, N. J., Procter, C. M., Connolly, E. L., and Guerinot, M. L. (1999) *Nature* **397,** 694–697
38. Dunlap, J. C. (1999) *Cell* **96,** 271–290
39. McWatters, H. G., Bastow, R. M., Hall, A., and Millar, A. J. (2000) *Nature* **408,** 716–720
40. Covington, M. F., Panda, S., Liu, X. L., Strayer, C. A., Wagner, D. R., and Kay, S. A. (2001) *Plant Cell* **13,** 1305–1315
41. Liu, X. L., Covington, M. F., Fankhauser, C., Chory, J., and Wagner, D. R. (2001) *Plant Cell* **13,** 1293–1304
42. Briat, J. F., Ravet, K., Arnaud, N., Duc, C., Boucherez, J., Touraine, B., Cellier, F., and Gaymard, F. (2009) *Ann. Bot. (Lond)* doi: mcp128 [pii]10.1093/aob/mcp128
43. Van Wuytswinkel, O., Vansuyt, G., Grignon, N., Fourcroy, P., and Briat, J. F. (1999) *Plant J.* **17,** 93–97
44. Ravet, K., Touraine, B., Kim, S. A., Cellier, F., Thomine, S., Guerinot, M. L., Briat, J.-F., and Gaymard, F. (2009) *Molecular Plant* doi:10.1093/mp/ssp041
45. Guerinot, M. L., and Yi, Y. (1994) *Plant Physiol.* **104,** 815–820
46. Blain, S., Queguiner, B., Armand, L., Belviso, S., Bombled, B., Bopp, L., Bowie, A., Brunet, C., Brussaard, C., Carlotti, F., Christaki, U., Corbiere, A., Durand, I., Ebersbach, F., Fuda, J. L., Garcia, N., Gerringa, L., Griffiths, B., Guigue, C., Guillerm, C., Jacquet, S., Jeandel, C., Laan, P., Lefevre, D., Lo Monaco, C., Malits, A., Mosseri, J., Obernosterer, I., Park, Y. H., Picheral, M., Pondaven, P., Remenyi, T., Sandroni, V., Sarthou, G., Savoye, N., Scouarnec, L., Souhaut, M., Thuiller, D., Timmermans, K., Trull, T., Uitz, J., van Beek, P., Veldhuis, M., Vincent, D., Viollier, E., Vong, L., and Wagener, T. (2007) *Nature* **446,** 1070–1074
47. Cassar, N., Bender, M. L., Barnett, B. A., Fan, S., Moxim, W. J., Levy, H., and Tilbrook, B. (2007) *Science* **317,** 1067–1070
48. Sanchez Villarreal, A., and Davis, S. J. (2009) TIME FOR COFFEE sets the circadian clock at dawn by integrating metabolic signals. In *20th International Conference on Arabidopsis Research*, Edinburgh, UK
49. Baena-Gonzalez, E., Rolland, F., Thevelein, J. M., and Sheen, J. (2007) *Nature* **448,** 938–942
50. Baena-Gonzalez, E., and Sheen, J. (2008) *Trends Plant Sci.* **13,** 474–482
51. Farras, R., Ferrando, A., Jasik, J., Kleinow, T., Okresz, L., Tiburcio, A., Salchert, K., del Pozo, C., Schell, J., and Koncz, C. (2001) *EMBO J.* **20,** 2742–2756
52. Baruah, A., Simkova, K., Apel, K., and Laloi, C. (2009) *Plant Mol. Biol.* **70,** 547–563
53. Baruah, A., Simkova, K., Hincha, D. K., Apel, K., and Laloi, C. (2009) *Plant J.* doi: TPJ3935 [pii]10.1111/j. 1365-313X. 2009.03935.x
54. Bhalerao, R. P., Salchert, K., Bako, L., Okresz, L., Szabados, L., Muranaka, T., Machida, Y., Schell, J., and Koncz, C. (1999) *Proc. Natl. Acad. Sci. U.S.A.* **96,** 5322–5327
55. Smith, A. M., and Stitt, M. (2007) *Plant Cell Environ.* **30,** 1126–1149
56. Moore, B., Zhou, L., Rolland, F., Hall, Q., Cheng, W. H., Liu, Y. X., Hwang, I., Jones, T., and Sheen, J. (2003) *Science* **300,** 332–336
57. Blasing, O. E., Gibon, Y., Gunther, M., Hohne, M., Morcuende, R., Osuna, D., Thimm, O., Usadel, B., Scheible, W. R., and Stitt, M. (2005) *Plant Cell* **17,** 3257–3281
58. Czechowski, T., Stitt, M., Altmann, T., Udvardi, M. K., and Scheible, W. R. (2005) *Plant Physiol.* **139,** 5–17